Erbium in GaAs: Coupling with native defects

Akihito Taguchi
NTT Basic Research Laboratories, 3-1 Morinosato Wakamiya, Atsugi-shi, Kanagawa 243-01, Japan

Takahisa Ohno
National Research Institute for Metals, 1-2-1 Sengen, Tsukuba-shi, Ibaraki 305, Japan
(Received 28 June 1996; revised manuscript received 24 June 1997)

We calculated the total energy of Er point defects in GaAs and of Er defects coupled with native defects in GaAs by the *ab initio* pseudopotential method. The total-energy calculation indicates that various coupled defects comprising an Er atom and native defects will be formed depending on the growth conditions and the Fermi-level position. By investigating the valence charge distribution, it was found that an Er atom forms a strong bond with an As atom. This chemical feature and the lattice relaxation around the coupled defect are the main factors that stabilize the coupled states. The intra-$4f$-shell luminescence spectrum of Er in GaAs is generally complicated and strongly depends on sample preparation methods and growth conditions. We propose that this tendency is due to the sample-dependent concentration of various defects that form complexes with Er. [S0163-1829(97)01039-4]

I. INTRODUCTION

Recently, rare-earth- (RE) doped semiconductors have received considerable attention, since RE ions emit sharp luminescence due to the RE intra-$4f$-shell transition. The luminescence wavelength is temperature stable since the RE $4f$-shell is well shielded by outer $5s$ and $5p$ electrons. RE-doped semiconductors may be useful in making optical devices. Among the many combinations of RE elements and semiconductors, Er-doped GaAs have been one of the most widely studied materials. This is because the wavelength of the luminescence due to the Er intra-$4f$-shell transition is about 1.54 μm, which corresponds to the minimum-loss wavelength region of silica-based fiber, and because it is possible to fabricate a good pn junction by using GaAs, which can be used as a carrier-injection optical device. The luminescence spectrum, however, strongly depends on the growth conditions; it shows that many kinds of Er luminescence centers with different atomic configurations are formed in a sample during growth.

Rutherford backscattering (RBS) has been widely used to investigate the lattice sites of atoms. The annealing effect of Er-ion-implanted GaAs samples has been investigated by RBS (Ref. 1) and it was reported that Er atoms move from interstitial sites to substitutional sites by annealing. In GaAs:Er samples grown by metalorganic chemical vapor deposition (MOCVD), the RBS measurement indicates that Er is at an interstitial site.[2] It was suggested that Er ions coupled with carbon atoms in these samples, because the concentrations of carbon and Er are nearly the same, and because the sample shows n-type conductivity although a high concentration of carbon is incorporated.[3] In GaAs there is only one Er luminescence center, whose atomic configuration has been well studied.[4] This Er luminescence center is formed when oxygen is co-doped with Er into GaAs by MOCVD. The center is composed of one Er atom and two oxygen atoms that occupy the nearest-neighbor sites of Er. However, the formation process and the atomic configurations of most Er luminescence centers in GaAs are not known.

Only one theoretical study, by Needels, Schlüter, and Lannoo, has been reported on the stable site of RE impurity in semiconductor hosts for Er in Si.[5] They calculated the cohesive energy for Er point defects at the tetrahedral and hexagonal interstitial sites and at the substitutional site. They concluded that the most stable case is that in which an Er^{3+} ion occupies the T_d interstitial site. However, the Er intra-$4f$-shell luminescence spectrum in Si is complicated and shows many luminescence lines, indicating the presence of many kinds of Er luminescence centers. Er seems to form complexes in Si like it does in GaAs.

In this paper, we discuss the stable configuration and the formation of Er centers in GaAs based on calculations of the total energies for Er-related defects in GaAs host. Since many kinds of Er luminescence centers are generally formed in GaAs, even in samples containing no extrinsic impurities and in samples with rather low Er concentration, we considered the coupling of Er atoms with native defects in GaAs. For several point defects, we discuss the charge state effect. For the coupled defects, we do not discuss the charge state effect in detail, since the atomic configurations are not clear for most Er luminescence centers, making it impossible to compare the calculated results with experiments. The charge state will become important in investigating the details of the formation processes when the configuration becomes clear. Therefore, we mainly discuss the more general features of Er in GaAs. In the next section, the calculation method is briefly explained. In Sec. III, the Er point defects are discussed. Er defects coupled with native defects are discussed in Sec. IV for As-rich and Ga-rich conditions. After the total energies are compared between the point defects and the coupled defects, the charge states are discussed for several defects. In Sec. V, the total valence charge distribution is shown in order to discuss the bonding nature of Er.

II. CALCULATION METHOD

The total-energy calculation was carried out within the local density-functional approach. The Wigner form of the exchange-correlation energy and *ab initio* norm-conserving

Kleinman-Bylander pseudopotentials were used.[6,7] The pseudo wave functions were expanded by a plane-wave basis set. The kinetic-energy cutoff was taken to be 8.41 Ry. A larger value of 16 Ry for the cutoff energy was used to check the convergence of the total-energy difference between different defects. The energy differences were less than 0.01 Ry. A 32-atom supercell was used, allowing relaxation of the first and second-nearest-neighbor atoms around a point defect. The conjugate-gradient technique was used to optimize both the electronic structure[8] and atomic configuration.[9]

To carry out the calculations, the *ab initio* pseudopotential for Er has to be determined. An Er atom might take two oxidation states: Er^{2+} and Er^{3+}. Here, ''Er^{2+}'' means the ground state of an isolated Er atom takes the electron configuration $[Xe]4f^{12}6s^2$, and ''Er^{3+}'' means it takes $[Xe]4f^{11}6s^25d^1$. The superscripts ''2'' and ''3'' in ''Er^{2+}'' and ''Er^{3+}'' are the number of valence electrons. The Er $4f$-shell luminescence from the GaAs host is due to the Er intra-$4f$-shell transition of the Er^{3+} oxidation state. In electron spin-resonance experiments for an n-type GaAs:Er sample, signals from the Er^{3+} state were observed,[10] indicating that an Er atom takes the 3+ oxidation state even in the n-type host. Therefore, most calculations have been done for the 3+ oxidation state of Er. Although the Er^{2+} state has not been experimentally observed in GaAs, we have checked the stability of $Er^{2+}$and Er^{3+} oxidation states in GaAs for some defect configurations by calculating the difference in the cohesive energy between the two oxidation states. The results will be shown later.

The Er^{3+} intra-$4f$-shell luminescence spectrum is very sharp, since the $4f$ shell is well-localized near the nucleus and shielded by outer $5s$ and $5p$ electrons. The sharp spectrum indicates a small interaction between the $4f$ shell and the host. Hence, the $4f$ shell was treated as the core in the determination of the Er pseudopotential. The same treatment on the construction of Er pseudopotential was adopted in the calculations for Er in Si.[5]

We checked the Er potential for the 3+ oxidation state by calculating the lattice constant and the electronic structure of ErAs. The calculated lattice constant is about 2% smaller than the value obtained experimentally.[11] This accuracy is nearly the same as that for GaAs.[12] The obtained electronic structure shows that ErAs is a semimetal, which is consistent with the experiments.[13] The obtained band dispersion relation is similar to that calculated by the linear muffin-tin orbital method.[14]

III. Er POINT DEFECTS

Ion implantation has been widely used to dope RE ions into semiconductor hosts, since the solubility of RE in semiconductors is very small. Annealing is usually carried out after implantation to recover the implantation damage and to obtain RE $4f$-shell luminescence. RBS experiments for Er-implanted GaAs samples have been reported.[1] The results suggest that Er atoms are moved from interstitial sites to substitutional sites by annealing. Hence, we considered the following two reactions and calculated the total energies:

$$\mathrm{Er}_{i(\mathrm{As})} \leftrightarrow \mathrm{Er}_{\mathrm{As}} + \mathrm{As}_{i(\mathrm{Ga})}, \tag{1a}$$

TABLE I. Total-energy difference for reactions (1a) and (1b). ΔE represents the total-energy difference between the left and right sides of the reactions. A negative value means that the total energy of the right side is smaller than that of the left side.

Eq. number	Reaction	ΔE (eV)
(1a)	$\mathrm{Er}_{i(\mathrm{As})} \leftrightarrow \mathrm{Er}_{\mathrm{As}} + \mathrm{As}_{i(\mathrm{Ga})}$	+6.61
(1b)	$\mathrm{Er}_{i(\mathrm{As})} \leftrightarrow \mathrm{Er}_{\mathrm{Ga}} + \mathrm{Ga}_{i(\mathrm{Ga})}$	−0.26

$$\mathrm{Er}_{i(\mathrm{As})} \leftrightarrow \mathrm{Er}_{\mathrm{Ga}} + \mathrm{Ga}_{i(\mathrm{Ga})}. \tag{1b}$$

Here, Er_{As} and Er_{Ga} are the Er atom at the As substitutional site and at the Ga substitutional site, respectively. $Er_{i(As)}$ is an Er atom at the interstitial site with T_d symmetry. The subscript ''As'' denotes the kind of atoms at the nearest-neighbor sites. In GaAs, there is another T_d interstitial site having Ga atoms as the nearest-neighboring atoms. Since the calculated total energy of $Er_{i(As)}$is smaller than that of $Er_{i(Ga)}$ by 0.28 eV, $Er_{i(As)}$ is used in Eqs. (1a) and (1b). For Ga and As, $Ga_{i(Ga)}$ and $As_{i(Ga)}$ were used, since we have found they are more stable than $Ga_{i(As)}$ and $As_{i(As)}$. The stabilities for Ga and As interstitials are the same as those previously calculated.[15]

As mentioned in the previous section, an Er atom might take two oxidation states: 2+ or 3+. We have confirmed that an Er atom takes the 3+ oxidation state in GaAs by calculating the difference in the cohesive energy between the 2+ and 3+ oxidation states for $Er_{i(As)}$. The cohesive energy difference, ΔE_{coh}, can be defined as[5]

$$\Delta E_{\mathrm{coh}} \equiv \mathrm{Er}^{3+}_{\mathrm{coh}} - \mathrm{Er}^{2+}_{\mathrm{coh}} = [E(\mathrm{Er}^{3+})_{\mathrm{psat}} - E(\mathrm{Er}^{2+})_{\mathrm{psat}}] - [E(\mathrm{Er}^{3+}_{i(\mathrm{As})}) - E(\mathrm{Er}^{2+}_{i(\mathrm{As})}] - [E(\mathrm{Er}^{3+}_{\mathrm{atom}}) - E(\mathrm{Er}^{2+}_{\mathrm{atom}})],$$

where psat means pseudoatom. The last term is the energy needed to move one electron from the $4f$ shell to the $5d$ shell in an atom. Since the correlation between $4f$ electrons is strong and then this energy is a many-body problem, the calculation of this energy is difficult. Hence, we used the experimentally measured energy of 0.89 eV to move electrons from the $4f^{12}6s^2$ multiplet to the $4f^{11}6s^25d^1$multiplet, as Needels, Schlüter, and Lannoo did.[5] The calculated ΔE_{coh} is +0.40 eV, confirming that an Er atom takes the 3+ oxidation state in GaAs. Hence, we used the Er pseudopotential for the 3+ oxidation state to calculate the reactions expressed by Eq. (1) and other reactions that will be presented later.

The calculated results for Eqs. (1a) and (1b) are shown in Table I, where ΔE denotes the total energy difference between the left and right sides of the reactions. A negative value means that the total energy of the right side is smaller than that of the left side. The value of ΔE is positive and large for reaction (1a), showing that an Er atom at the As site is unstable. On the other hand, for Eq. (1b), the ΔE is negative, suggesting that $Er_{i(As)}$ probably moves to the Ga lattice site, and then the Ga atom moves to the T_d interstitial site surrounded by Ga atoms. Thus, reaction (1b) may occur when Er-implanted GaAs samples are annealed. This is consistent with the experimentally observed results in RBS.[1]

Since the ion radius of Er is much larger than that of Ga and As, the stress around Er ions in GaAs must be very large.

The calculated results show that the nearest-neighboring atoms move significantly outward. In the substitutional case, Er_{Ga}, the Er-As distance is about 5.9% larger than the Ga-As distance. In the interstitial case, $Er_{i(As)}$, the distance between the Er atom and the nearest-neighbor As atom extends by about 3.1% compared with the unrelaxed case.

IV. Er COUPLED DEFECTS WITH OTHER POINT DEFECTS

The calculated results for Er defects suggest that the Ga substitutional site is stable. However, if this site were dominant in GaAs, it would not explain the fact that many kinds of Er luminescence centers are generally formed during the growth of GaAs:Er samples. In the previous section, it was assumed that Er interstitials are formed by the ion implantation. During crystal growth, however, both substitutional and interstitial Er will be formed and several kinds of native defects will also be formed. Hence, in this section, we consider Er coupled with native defects in GaAs under As-rich and Ga-rich conditions. Er-to-Er coupling will also be considered. After that, the charge state effect on the reactions is discussed for several reactions.

A. As-rich condition

GaAs samples are usually grown under As-rich conditions by metalorganic chemical phase epitaxy and molecular-beam epitaxy. Under As-rich conditions, native defects, such as a Ga vacancy (V_{Ga}), As interstitial (As_i), As antisite (As_{Ga}), and a coupled defect of an As antisite and an As vacancy ($\{As_{Ga}-V_{As}\}$) will be formed.[15,18] Reactions between these four native defects and Er point defects were considered. Er_{Ga} and $Er_{i(As)}$ were used as the Er point defects, because Er_{Ga} is more stable than Er_{As}, and $Er_{i(As)}$ is more stable than $Er_{i(Ga)}$, as shown in the previous section. We considered the following reactions:

$$V_{Ga}+Er_{i(As)}\leftrightarrow Er_{Ga}, \tag{2a}$$

$$As_{i(Ga)}+Er_{Ga}\leftrightarrow\{Er_{Ga}-As_{i(Ga)}\}, \tag{2b}$$

$$As_{Ga}+Er_{i(As)}\leftrightarrow\{As_{Ga}-Er_{i(Ga)}\}, \tag{2c}$$

$$\{As_{Ga}-V_{As}\}+Er_{i(As)}\leftrightarrow Er_{Ga}. \tag{2d}$$

Eight reactions can be considered between the four kinds of native defects and the two kinds of Er point defects. However, we will only discuss some of those shown in Eq. (2). The coupled defects in these reactions are composed of point defects located at the nearest-neighbor sites. Defects coupled with two atoms at the second-nearest-neighbor sites, for example $\{Er_{Ga}-As_{As}-As_{Ga}\}$, were not considered, since such defects are too large to be treated within the 32-atom supercell. Even for the coupled defects in Eq. (2), the lattice around the coupled defects can not be fully relaxed. However, to relax the nearest- and second-nearest-neighboring atoms of the coupled defect, a larger unit cell and more calculation time are required. To avoid a huge amount of calculation and still obtain reasonable results by using the 32-atom supercell, the positions of the atoms neighboring the coupled defect were determined on the basis of calculations for each point defect.

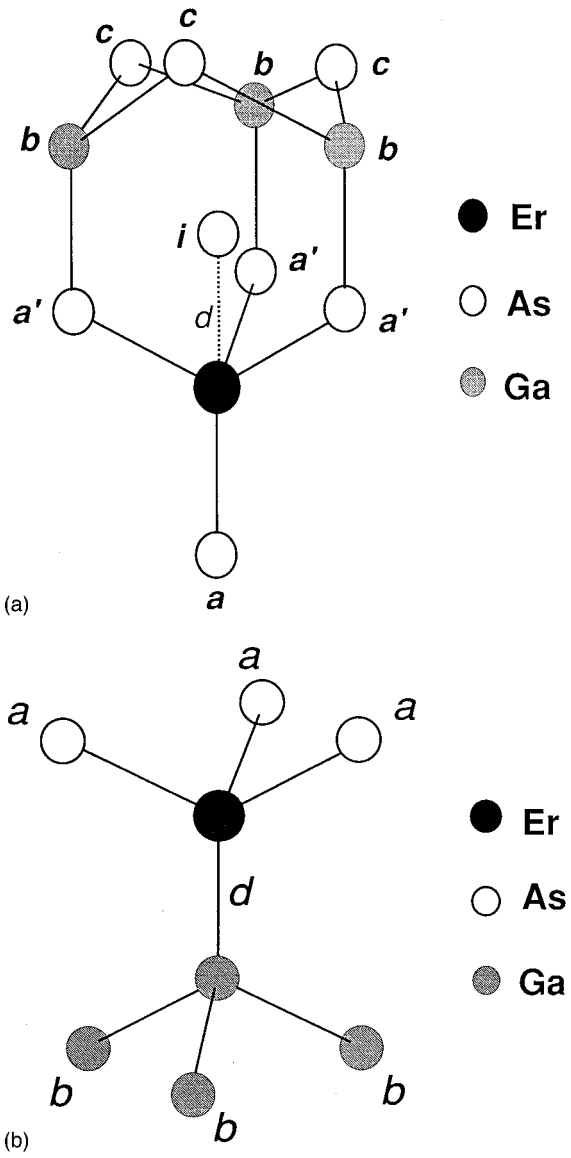

FIG. 1. (a) Atomic configurations of the coupled defect of Er_{Ga} and $As_{i(Ga)}$. The As T_d interstitial defect is denoted by i. The a and a' atoms are the atoms nearest to Er_{Ga}. a' atoms are also the second-nearest-neighboring atoms to $As_{i(Ga)}$. The b and c atoms are the nearest- and the second-neighboring atoms to $As_{i(Ga)}$, respectively. Er_{Ga}, a, and a' atoms are considered as one group, and $As_{i(Ga)}$, b and c as another group. The distance d between the two-atom groups was changed to obtain the stable structure. (b) Atomic configurations of the coupled defect of Er_{Ga} and Ga_{As}. The a and b atoms are the nearest-neighboring atoms to Er_{Ga} and Ga_{As}, respectively. Er_{Ga} and a atoms are considered as one group, and Ga_{As} and b atoms as another group. By changing d, which is the distance between the two groups, the total energy was minimized.

Figure 1(a) shows a schematic atomic configuration of the coupled defect $\{Er_{Ga}-As_{i(Ga)}\}$. An Er atom is at the Ga substitutional site and an As atom occupies the nearest-neighbor T_d interstitial site, which is denoted by i. The atoms neighboring the coupled defect are denoted by a, a', b, and c. For these atoms, the lattice relaxation was taken into ac-

TABLE II. Total-energy difference for reactions (2a) to (2d) for the As-rich condition.

Eq. number	Reaction	ΔE (eV)
(2a)	$V_{Ga}+Er_{i(As)}\leftrightarrow Er_{Ga}$	−4.75
(2b)	$As_{i(Ga)}+Er_{Ga}\leftrightarrow\{Er_{Ga}-As_{i(Ga)}\}$	−0.32
(2c)	$As_{Ga}+Er_{i(As)}\leftrightarrow\{Er_{i(Ga)}-As_{Ga}\}$	−0.11
(2d)	$\{As_{Ga}-V_{As}\}+Er_{i(As)}\leftrightarrow Er_{Ga}$	−5.00

count, and the positions of the outer atoms were fixed at the ideal GaAs lattice sites. For the a and a' atoms, the interactions with the Er_{Ga} defect should be stronger than those with the $As_{i(Ga)}$ defect, since the a' atoms are closer to Er_{Ga}, than they are to $As_{i(Ga)}$. Hence, the positions of these atoms were determined from the calculated results for the Er_{Ga} point defect; that is, the distance between the a (a') atom and the Er defect was taken to be equal to the distance obtained in the Er_{Ga} point defect calculations. For the b and c atoms, the positions obtained in the calculations for the $As_{i(Ga)}$ point defect were used, since the interactions with the $As_{i(Ga)}$ defect should be stronger than the interactions with the Er_{Ga} defect. We considered the Er_{Ga}, a, and a' atoms to be one group, and the $As_{i(Ga)}$, b, and c atoms to be another group. Then, the distance between the two groups, d, was changed so as to give the minimum total energy.

For the case in which two point defects are at the substitutional sites, the lattice relaxation was considered as follows. Figure 1(b) shows an example of coupled defects Er_{Ga} and Ga_{As}. The a and b atoms are the atoms nearest of Er_{Ga} and Ga_{As}, respectively. The relative positions of $a(b)$ atoms and Er_{Ga} (Ga_{As}) were obtained from the calculated results for the isolated Er_{Ga} (Ga_{As}) point defect. The positions of the atoms surrounding the coupled defect were fixed at the ideal GaAs lattice sites. In this case, we considered Er_{Ga} and the a atoms to be one group, and Ga_{As} and the b atoms to another group. The total energy was minimized by changing the distance between the two groups.

The calculated results for the As-rich condition are summarized in Table II. The definition of ΔE is the same as that used in Table I. For the reaction between V_{Ga} and $Er_{i(As)}$ [Eq. (2a)], it is expected that an Er ion occupies the Ga site, since V_{Ga} has dangling bonds that enlarge the total energy. The calculated result indeed shows that Er_{Ga} is more stable.

Equation (2b) considers the coupling between Er at the Ga substitutional site and As at the T_d interstitial site. The calculated results show that the coupled state, $\{Er_{Ga}-As_{i(Ga)}\}$, is more stable than the separated state, $As_{i(Ga)}+Er_{Ga}$. In the calculations of each point defect, the nearest- and second-nearest atoms were relaxed, while in the calculations of the coupled defect the lattice relaxation effect was partially included as previously explained. Therefore, the total energy of the coupled defect should be smaller when the lattice is fully relaxed. The exact value of the energy reduction due to the full lattice relaxation of the coupled defect was not obtained, but it would be in the range of 0.4–1.4 eV, providing the lattice relaxation effect is similar to that for the point defect. Hence, the total-energy difference should be larger than the listed value for this reaction.

The reaction between the As antisite and the Er interstitial defects is described in Eq. (2c). The value obtained for ΔE is small and negative. When the lattice relaxation of the coupled defect due to the change in distance d is not included, ΔE is small and positive.[19] Hence, the coupled defect $\{As_{Ga}-Er_{i(Ga)}\}$ is stabilized by the lattice relaxation.

For the reaction between $\{As_{Ga}-V_{As}\}$ and $Er_{i(As)}$ expressed by Eq. (2d), there is a possibility that an Er atom occupies the As lattice site. However, $\{Er_{Ga}-As_{As}\}$ ($\equiv Er_{Ga}$) must be more stable than $\{As_{Ga}-Er_{As}\}$, since Er tends to occupy the Ga lattice site and As is definitely stable at the As lattice site. The total energy of $\{As_{Ga}-V_{As}\}$ becomes smaller when the lattice is fully relaxed. The amount of the energy reduction is expected to be 0.4–1.4 eV; that is, smaller than the absolute value of ΔE for the reaction described by Eq. (2d). Hence, Er_{Ga} is more stable, even when the lattice is fully relaxed.

The results for reactions (2a) and (2d) suggest that Er_{Ga} is easily formed. When As interstitial atoms are contained in GaAs samples, they may couple with Er_{Ga}, resulting in the formation of the coupled defect $\{Er_{Ga}-As_{i(Ga)}\}$. When As_{Ga} is present, it couples with $Er_{i(As)}$, forming another coupled defect. Thus, an Er atom becomes stable by coupling with an excess As atom in GaAs.

B. Ga-rich condition

For the Ga-rich condition, the following native defects will be formed in analogy with the As-rich condition: an As vacancy (V_{As}), Ga interstitial (Ga_i), Ga antisite (Ga_{As}), and a coupled defect of a Ga antisite and a Ga vacancy ($\{Ga_{As}-V_{Ga}\}$).[15] The reactions of these four native defects with the Er point defects Er_{Ga} and $Er_{i(As)}$ were considered for the Ga-rich condition. Here, the reaction between Er_{As} and $Ga_{i(Ga)}$ is also considered in Eq. (3g), since reaction (3a) indicates the possibility of Er_{As} formation. Thus, the following seven reactions were considered:

$$V_{As}+Er_{i(As)}\leftrightarrow Er_{As}, \tag{3a}$$

$$V_{As}+Er_{Ga}\leftrightarrow\{Er_{Ga}-V_{As}\}, \tag{3b}$$

$$Ga_{i(Ga)}+Er_{Ga}\leftrightarrow\{Er_{Ga}-Ga_{i(Ga)}\}, \tag{3c}$$

$$Ga_{As}+Er_{i(As)}\leftrightarrow\{Er_{i(As)}-Ga_{As}\}, \tag{3d}$$

$$Ga_{As}+Er_{Ga}\leftrightarrow\{Er_{Ga}-Ga_{As}\}, \tag{3e}$$

$$\{Ga_{As}-V_{Ga}\}+Er_{i(As)}\leftrightarrow\{Er_{Ga}-Ga_{As}\}, \tag{3f}$$

$$Ga_{i(Ga)}+Er_{As}\leftrightarrow\{Er_{i(As)}-Ga_{As}\}. \tag{3g}$$

The calculation procedures were the same as those used for the As-rich conditions.

The results are summarized in Table III. Only one reaction, Eq. (3e), gives a positive value of ΔE. Since the total energy of the coupled defect becomes small when the lattice relaxation is fully included, as we described before, the actual value of ΔE may be small and possibly negative. All other values of ΔE in the table are negative, suggesting that the coupled states involving an Er atom and a native defect are generally more stable than the separated states.

Reaction (3a) shows that the Er interstitial defect will couple with V_{As}, resulting in Er_{As}. However, Er_{As} may

TABLE III. Total-energy difference for reactions (3a) to (3g) for the Ga-rich condition.

Eq. number	Reaction	ΔE (eV)
(3a)	$V_{As}+Er_{i(As)}\leftrightarrow Er_{As}$	−1.13
(3b)	$V_{As}+Er_{Ga}\leftrightarrow\{Er_{Ga}-V_{As}\}$	−0.79
(3c)	$Ga_{i(Ga)}+Er_{Ga}\leftrightarrow\{Er_{Ga}-Ga_{i(Ga)}\}$	−0.02
(3d)	$Ga_{As}+Er_{i(As)}\leftrightarrow\{Er_{i(As)}-Ga_{As}\}$	−1.88
(3e)	$Ga_{As}+Er_{Ga}\leftrightarrow\{Er_{Ga}-Ga_{As}\}$	+1.09
(3f)	$\{Ga_{As}-V_{Ga}\}+Er_{i(As)}\leftrightarrow\{Er_{Ga}-Ga_{As}\}$	−2.42
(3g)	$Ga_{i(As)}+Er_{As}\leftrightarrow\{Er_{i(As)}-Ga_{As}\}$	−3.70

couple with $Ga_{i(Ga)}$ [reaction (3g)]. Er_{Ga} may form coupled defects with V_{As}, $Ga_{i(Ga)}$, and Ga_{As}. Hence, four kinds of coupled defects, $\{Er_{Ga}-V_{As}\}$, $\{Er_{Ga}-Ga_{i(Ga)}\}$, $\{Er_{i(As)}-Ga_{As}\}$, and $\{Er_{Ga}-Ga_{As}\}$, may be formed under the Ga-rich condition.

C. Er-Er coupling

When the Er concentration is high, reactions between Er atoms may be possible. We considered, as one example, the reaction

$$Er_{Ga}+Er_{i(As)}\leftrightarrow\{Er_{Ga}-Er_{i(Ga)}\}. \quad (4)$$

The calculated total energy of the coupled state of $\{Er_{Ga}-Er_{i(Ga)}\}$ is 0.37 eV lower than that for the separated state, suggesting that Er will form complexes when the Er concentration is high.

D. Charge state effect

In the above reactions, each defect is assumed to be neutral, but it is known that native defects take several charge states depending on the Fermi-level position.[15–17] The Er defects may also take several charge states depending on the Fermi level. Hence, the total-energy difference ΔE in the tables depends on the Fermi level. Here, we discuss this Fermi-level effect for reactions (2a) and (3a). In this paper, we do not discuss the effect in details for the other reactions, which include the coupled defects. For the coupled defects, we considered the lattice relaxation effect in a limited way, as explained in Figs. 1(a) and (b), and the charge state affects the lattice relaxation and the total energy. At present, the atomic structure of coupled defects comprising an Er atom and native defects are not known. Therefore, a detailed investigation of the charge state of such coupled defects remains as future work.

To investigate the total-energy difference as a function of the Fermi level, which is called the reaction energy,[15] the dependence of the total energy on the Fermi level has to be known for the defects in each charge state (the formation energy[15,16]). The calculated formation energies as a function of the Fermi level are, respectively, shown in Figs. 2, 3, and 4, for $Er_{i(As)}$, Er_{Ga}, and V_{Ga}, which are included in the reaction (2a), $V_{Ga}+Er_{i(As)}\leftrightarrow Er_{Ga}$. Up to the second-nearest-neighbor atoms were relaxed at each charge state. The total energy for the neutral charge state was taken as the energy reference for each point defect. The Fermi level was measured by the calculated band-gap energy. For $Er_{i(As)}$, the formation energy for the 2+ charge state is lower than that for the 1+ and 0 charge states at any Fermi-level position, showing that the 2+ charge state is the most stable state for any Fermi level. For Er_{Ga}, the neutral charge state is most stable for almost all Fermi-level positions, and Er_{Ga} acts as

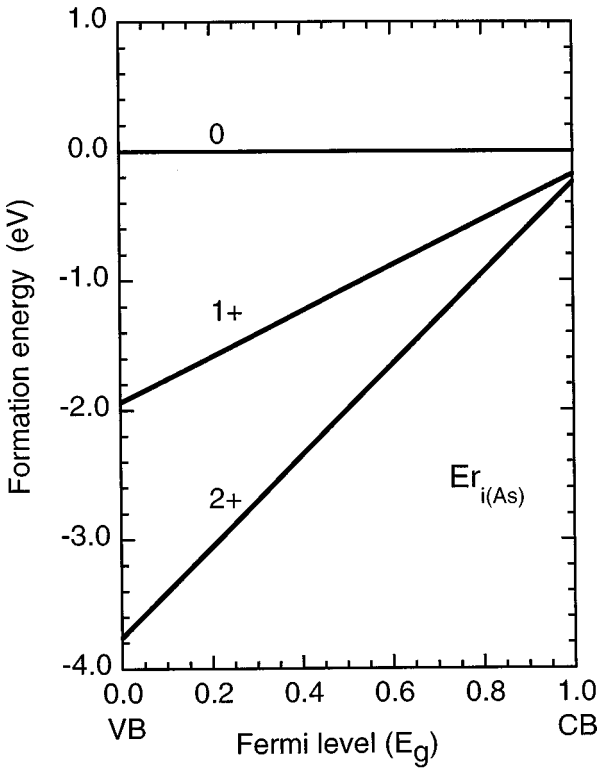

FIG. 2. Formation energy of $Er_{i(As)}$. The horizontal axis is the Fermi level measured by the calculated band gap of GaAs. The neutral charge state was taken as an energy reference. The 2+ charge state is most stable for any Fermi level, ''0,'' ''1+,'' and ''2+'' denote the charge state.

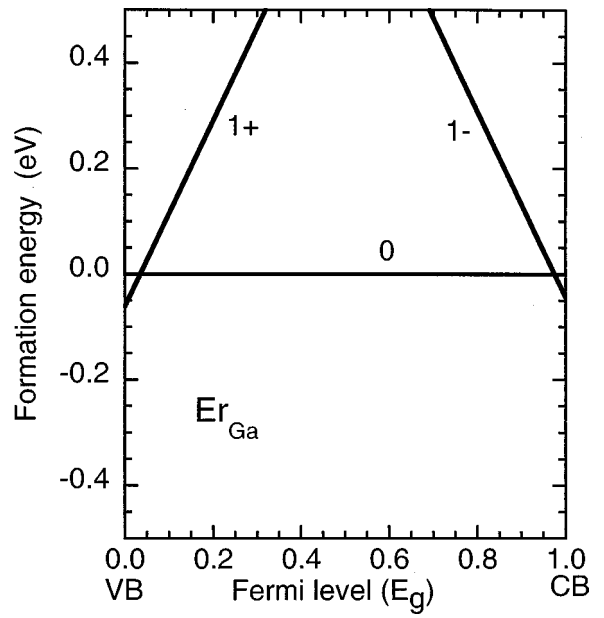

FIG. 3. Formation energy of Er_{Ga} as a function of the Fermi level. The neutral charge state was taken as the energy reference. At almost all Fermi-level positions, the neutral state is most stable.

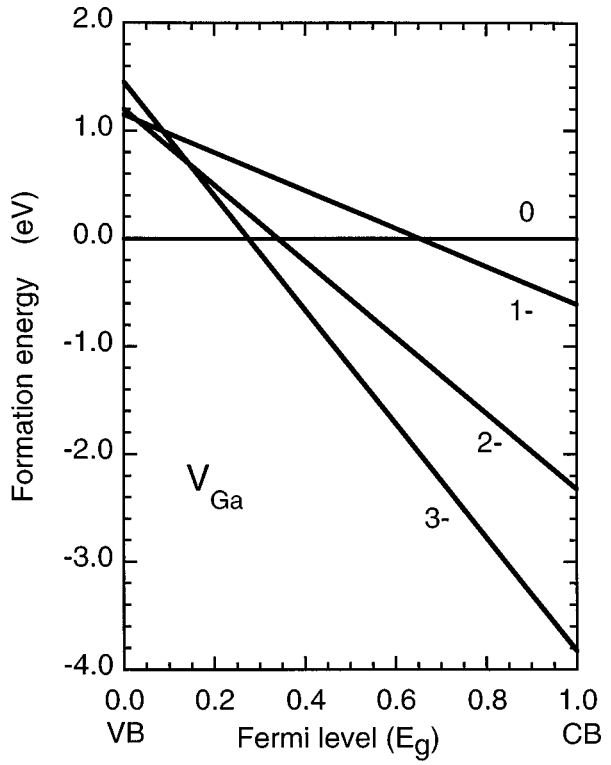

FIG. 4. Formation energy of V_{Ga} as a function of the Fermi level.

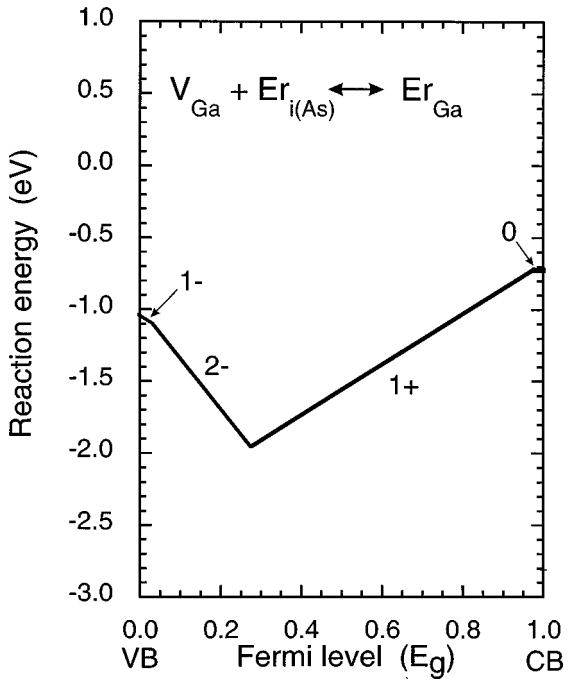

FIG. 5. Reaction energy for the reaction, $V_{Ga}+Er_{i(As)}\leftrightarrow Er_{Ga}$, as a function of the Fermi level. At any Fermi level, the reaction energy is negative, showing that Er_{Ga} is more favorable than the separated state, $V_{Ga}+Er_{i(As)}$.

both a shallow donor and a shallow acceptor. Several groups have calculated and reported the formation energy for V_{Ga}.[15–17] According to the reported results, V_{Ga} takes four charged states from 0 to 3−, while the present calculation results suggest that only 0 and 3− charged states may appear (Fig. 4). However, in the previously reported calculations, unlike the present case, the lattice relaxation around V_{Ga} was not taken into account. This may be the main reason for the difference between the reported results and the present results.

From the charge state dependence on the Fermi level of V_{Ga}, $Er_{i(As)}$, and Er_{Ga}, the reaction energy as a function of the Fermi level was calculated, and the results are shown in Fig. 5. The numbers in the figure indicate the charge difference during the reaction. For example, ''1+'' means that the total charge of the left-hand side of the reaction, $V_{Ga}+Er_{i(As)}$, is larger by one than that of the right-hand side, Er_{Ga}. At any Fermi level, the formation energy is negative, showing that Er_{Ga} is more stable than the separated state of V_{Ga} and $Er_{i(As)}$. Since the calculated results (Figs. 2 and 4) show that $Er_{i(As)}$ is a donor and that V_{Ga} is an acceptor, the charge states are more stable than the neutral states. As a result, the reaction energy increases. Hence, the formation energy values are closer to zero than the ΔE value shown in Table II.

To obtain the reaction energy of reaction (3a), $V_{As}+Er_{i(As)}\leftrightarrow Er_{As}$, the formation energies for Er_{As} and V_{As} were calculated, and the results are shown in Figs. 6 and 7. For Er_{As}, five charge states from 2+ to 2− may appear. Like for V_{Ga}, the formation energy for V_{As} has been calculated by several groups, but the results differ. Two charge states, 2+ and 1+, were suggested by Baraff and Schlüter.[15] Jansen and Sanke suggested three charge states from 1+ to 1−, and only 1+ charge state was also suggested.[17] The present calculations suggest three charge states from 2+ to 0.

Based on the calculated formation energies for V_{As}, $Er_{i(As)}$, and Er_{As}, the reaction energy for reaction (3a) was

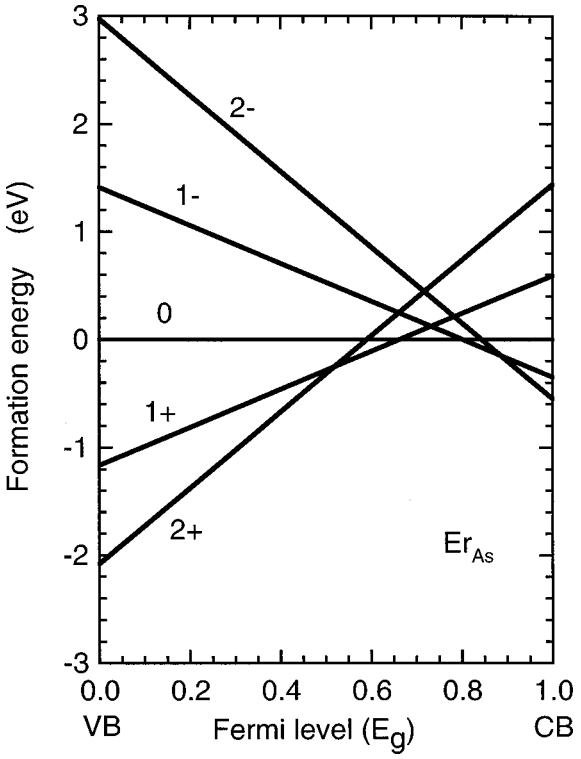

FIG. 6. Formation energy of Er_{As} as a function of the Fermi level. Five charge states from 2+ to 2− may appear depending on the Fermi level.

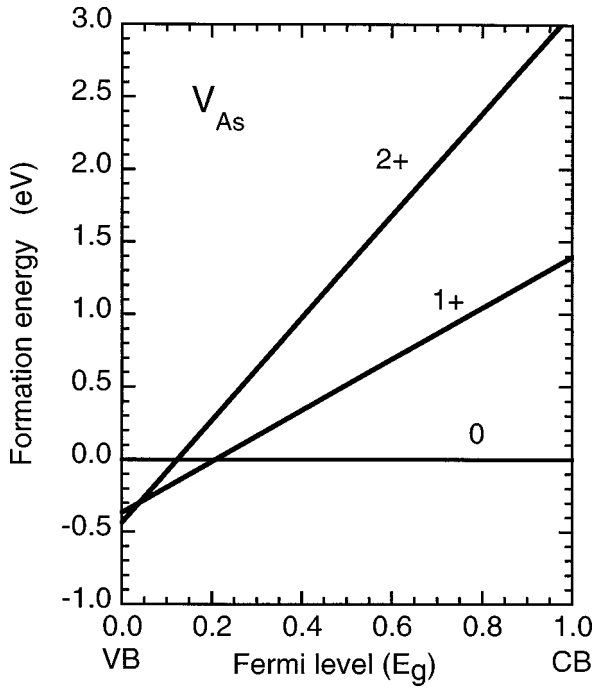

FIG. 7. Formation energy of V_{As} as a function of the Fermi level.

calculated, and the results are shown in Fig. 8. When the Fermi level is close to the top of the valence band, the reaction energy is positive. This means that the separated state, $V_{As}+Er_{i(As)}$, is more stable than Er_{As}, and this is contrary to the results shown in Table III. However, as the Fermi level approaches the bottom of the conduction band, the formation energy decrease, and then it becomes negative, indicating Er_{As} is more stable than the separated state. When the Fermi level is close to the top of the valence band, the positively charged state is most stable for Er_{As}. This reduces the total energy and then reduces the reaction energy, by about 2.1 eV. For V_{As} and Er_{iAs}, the positively charged states are also the most stable states when the Fermi level is close to the top of the valence band. However, this nature enlarges the reaction energy, which is opposite to the Er_{As} case. The reaction energy is enlarged by about 4.2 eV, which is larger than the sum of ΔE (Table III) and the reaction energy reduction of Er_{As} (2.1 eV). As a result, the reaction energy becomes positive at the top of the valence band. As the Fermi level rises, the formation energy of $Er_{i(As)}$ rises (Fig. 2). This results in the decrease in the reaction energy as the Fermi level rises.

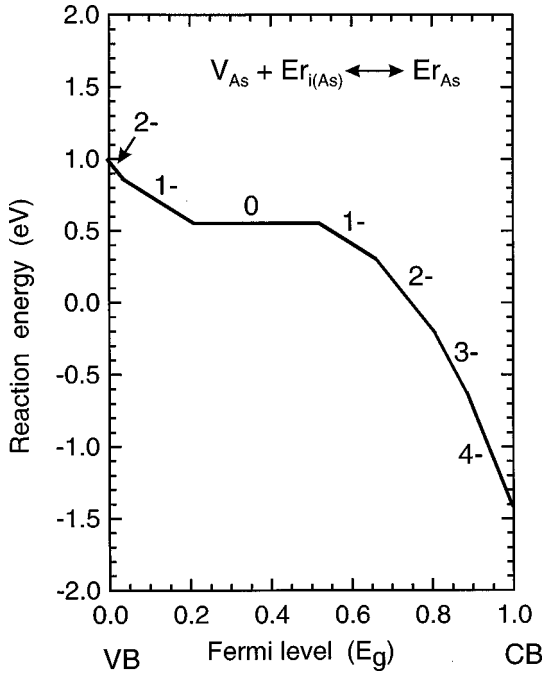

FIG. 8. Reaction energy of the reaction, $V_{As}+Er_{i(As)}\leftrightarrow Er_{As}$, as a function of the Fermi level. The reaction energy is positive at the top of the valence band, but it reduces as the Fermi level rises.

When a donor is included in the left-hand side of a reaction, the reaction energy becomes larger than that estimated from the neutral charge state, but the reaction energy decreases as the Fermi level moves from the top of the valence band to the bottom of the conduction band. An acceptor included in the left-hand side of a reaction also enlarges the reaction energy, but the reaction energy decreases as the Fermi level rises, which is opposite to the donor case. Based on these features, we can predict the dependence of the reaction energy on the Fermi level. We here consider the reactions (2b), (3b), and (3c) as examples. Considering reaction (2b), $As_{i(Ga)}+Er_{Ga}\leftrightarrow\{Er_{Ga}-As_{i(Ga)}\}$, it was reported that $As_{i(Ga)}$ is a donor,[15–17] and the present calculations show that Er_{Ga} is neutral for almost all Fermi-level positions. Hence, the formation energy decreases as the Fermi level rises. Although the formation energies for $As_{i(Ga)}$ and $\{Er_{Ga}-As_{i(Ga)}\}$ were not calculated and thus the exact values are not known, the coupled state might become stable when the Fermi level is close to the bottom of the conduction band, since ΔE (Table II) is negative, i.e., -0.32 eV. For reaction (3b), $V_{As}+Er_{Ga}\leftrightarrow\{Er_{Ga}-V_{As}\}$, the donor nature of V_{As} is -0.43 eV, which is larger than the ΔE value of -0.79 eV (Table III). Therefore, even at the top of the valence band, the formation energy must be negative, and it decreases as the Fermi level rises. Therefore, at any Fermi-level position, the reaction energy must be negative, and thus the coupled state is always more stable in this reaction. For reaction (3c), $Ga_{i(Ga)}+Er_{Ga}\leftrightarrow\{Er_{Ga}-Ga_{i(Ga)}\}$, since the ΔE value is close to zero as can be seen in Table III and $Ga_{i(Ga)}$ is a donor,[15–17] the coupled state might be stable only when the Fermi level is close to the bottom of the conduction band.

Since the reaction energy depends on the Fermi level, the ΔE values listed in the tables are not always the proper values for describing the reactions. However, these values can be used as guides to estimate the dependence of the reaction energy on the Fermi level. The calculated results for ΔE listed in the tables and the above discussions of the Fermi-level effect suggest that many kinds of coupled defects comprising an Er atom and native defects will be formed depending on the growth condition (whether it is As-rich or Ga-rich) and on the Fermi-level position. Therefore, even when the Er concentration is low, some kinds of coupled defects will be formed, and those defects are responsible for the complicated luminescence spectra. When the Er concentration is high, Er-Er coupled defects will also be formed and further coupling of Er-Er defects with native defects may occur. The concentrations of these coupled defects would depend on the sample preparation method, the growth con-

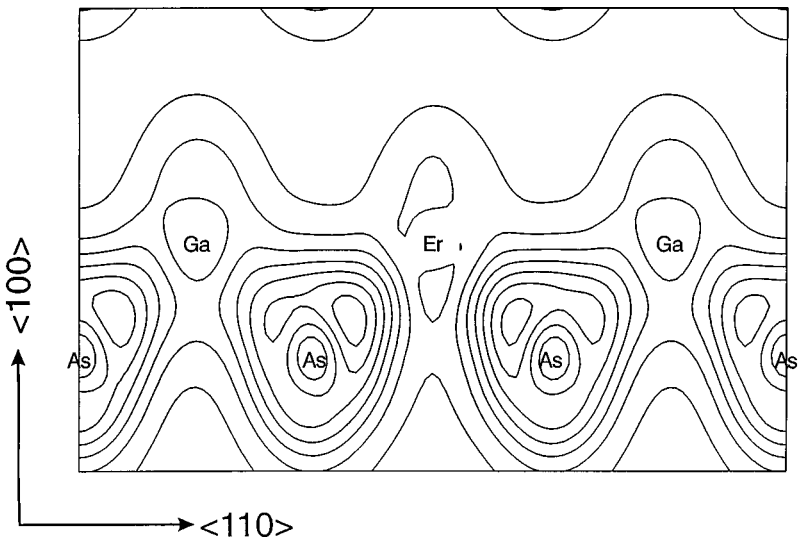

FIG. 9. Total valence charge distribution for Er_{Ga} on the (110) plane. ''Ga,'' ''As,'' and ''Er'' represent the kinds of elements and their positions. Between Ga and As, high charge-density regions are clearly seen, indicating the sp^3 hybridized orbitals. Similar high charge-density regions are seen between Er and As.

ditions, the host quality, and the Fermi level, resulting in the experimentally observed sample-dependent Er intra-$4f$-shell luminescence spectrum.

V. VALENCE CHARGE DISTRIBUTION

In the previous section, we showed that some coupled defects will form depending on the growth conditions and the Fermi-level position. In this section, we discuss the mechanisms by which the coupled defects are stabilized. A stable compound of Er and As is ErAs, which has the sodium-chloride structure with the coordination number of six, which is larger than the coordination number of four for the zinc-blende structure. Therefore, the bonding nature between Er and As atoms in GaAs and between these atoms in ErAs is very different. This may be one reason why the Er coupled defects are stable in GaAs. Another reason must be the fact that the radius of an Er atom is much larger than that of a Ga or As atom. The incorporated Er atom thus causes a large local stress, which may be reduced by coupled defect formation. The bonding nature and the lattice relaxation effect was examined by investigating the valence charge distribution. The valence charge distribution was calculated for the neutral state.

Figure 9 shows the valence charge distribution for Er_{Ga} on a (110) plane. Ga-As bonds can be clearly seen as the high charge density regions between them. Between Er and As, a similar high charge-density region can be clearly seen, showing that Er and As form a sp^3-like bond. The maximum charge density of the Er-As bond is larger than that of the Ga-As bond, and the charge density around an Er atom is lower than that of a Ga atom. These features may be the reason that the Er ion radius is larger than the Ga ion radius. When the interstitial Er atom goes into the Ga site in reaction (1b), Ga-As bonds have to be broken and then Er-As bonds are formed by changing $Er_{i(As)}$ to Er_{Ga}. The Ga atom goes into the interstitial site. The lattice stress around $Ga_{i(Ga)}$ must be smaller than that around $Er_{i(As)}$, but Er_{Ga} which is included in the right side of Eq. (1b), also causes local stress. Thus, if only lattice relaxation is considered, it seems that the formation of Er_{Ga} is not very favorable. However, the calculation shows that Er_{Ga} is more stable than $Er_{i(As)}$ meaning that Er-As bond formation reduces the total energy. This indicates that the Er-As bond is strong.

The charge distribution when an Er ion is at the T_d interstitial site surrounded by As atoms at the nearest-neighbor sites is shown in Fig. 10. Charges around As atoms at the

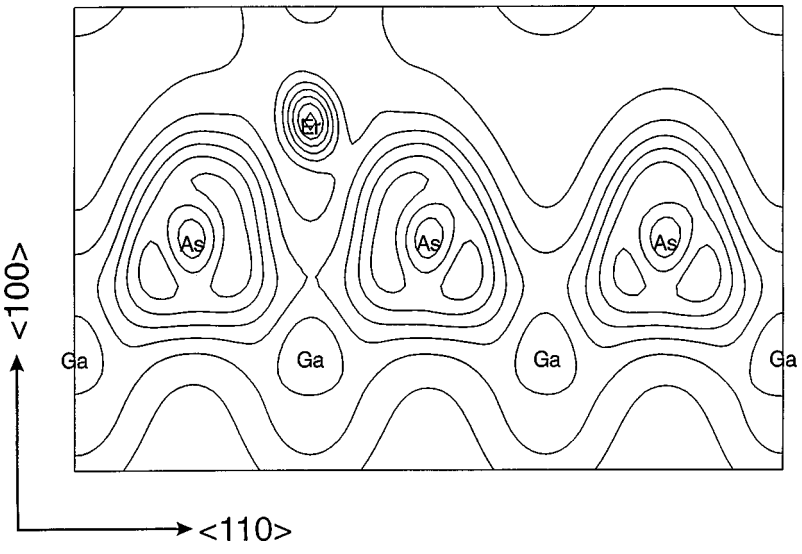

FIG. 10. the total valence charge distribution for an Er atom at the T_d interstitial site surrounded by As atoms at the first-nearest-neighbor sites. The charge localization around the Er atom is clearly seen.

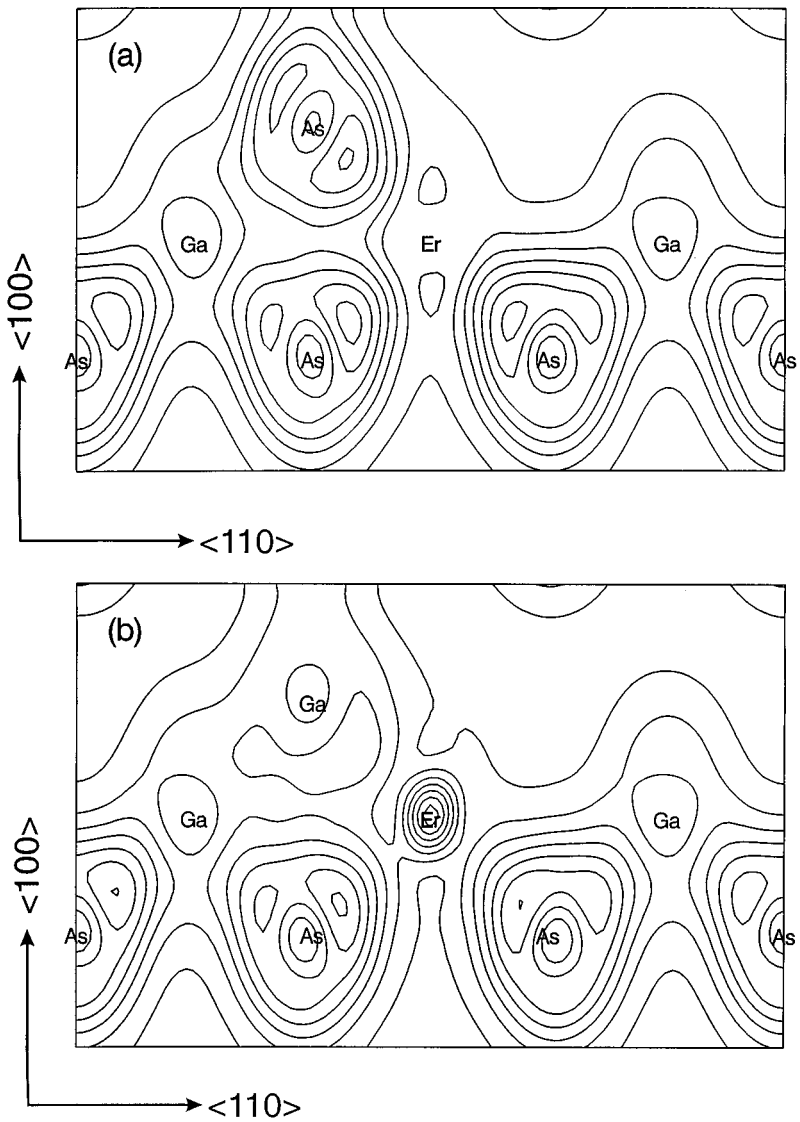

FIG. 11. Total valence charge distributions for (a) the coupled defect of $\{Er_{Ga}-As_{i(Ga)}\}$ and (b) the coupled defect of $\{Er_{Ga}-Ga_{i(Ga)}\}$. The bond can be seen between $As_{i(Ga)}$ and Er_{Ga}. The bond between Er_{Ga} and $Ga_{i(Ga)}$ is not clear. There is a localized charge around Er_{Ga}, which is similar to that in Fig. 3.

nearest-neighbor sites attract the Er atom, but the bond between Er and As seems to be weak compared with the Er_{Ga} case shown in Fig. 9. Charge localization around $Er_{i(As)}$ is clearly seen. Such charge localization is not seen in the Er_{Ga} case. The valence orbitals of an Er^{3+} ion are $6s$, $6p$, and $5d$. The $5d$ level is energetically lower than the $6p$ level. In semiconductor hosts, the formation of the sp^3 hybridized orbital reduces the total energy that is seen in the Er_{Ga} case. If Er does not form the sp^3 hybridized orbital, the three valence electrons of an Er^{3+} ion should be distributed among $6s$, $5d$, and $6p$ orbitals. $Er_{i(As)}$ must be such a case, and the localized charge around the Er atom must be due to the Er $5d$ orbital.

A comparison between reactions (2b) and (3c) shows the difference in the reaction of Er_{Ga} with As and Ga atoms at the interstitial site. The valence charge distribution for the $\{Er_{Ga}-As_{i(Ga)}\}$ coupled defect is shown in Fig. 11(a). In this case, the Er_{Ga} atom forms a bond with $Er_{i(Ga)}$. Since Er ions have a larger radius than Ga ions, the lattice stress is enlarged by forming the coupled defect. However, the total-energy calculation shows that the coupled defect is more stable. Hence, the Er-As bond is strong enough to compensate for the increase in the stress, resulting in a stable coupled defect. Figure 11(b) shows the valence charge distribution for the $\{Er_{Ga}-Ga_{i(Ga)}\}$ coupled defect. No bond can be seen between the Er atom and the interstitial Ga atom, and the localized charge is seen around the Er atom. In this case, it seems that the charge transfer to the Er $5d$ orbital stabilizes the defect.[20] The amount of the total energy decrease due to the coupled defect formation is larger in reaction (2b) than in (3c). This seems to be consistent with the consideration that the Er-As bond is strong.

Both reactions (3d) and (3e) are reactions of Ga_{As} with an Er atom, but in reaction (3d) Er occupies interstitial sites, while in reaction (3d) it occupies the Ga substitutional site. The coupled defect of $\{Ga_{As}-Er_{i(As)}\}$ is stable, but $\{Ga_{As}-Er_{Ga}\}$ is not stable. Figure 12(a) shows the valence charge distribution for $\{Ga_{As}-Er_{i(As)}\}$. Comparing this figure with Fig. 10 for $Er_{i(As)}$, one can see that the charge distribution around Er is similar. Hence, the coupled defect may be stabilized by the relaxation of the stress around the Er atom when the nearest-neighbor atom changes from As to Ga. Figure 12(b) shows the charge distribution of $\{Ga_{As}-Er_{Ga}\}$. The charge distribution around the Er atom is completely different from that shown in Fig. 9 for Er_{Ga}. To form a coupled defect, one of the Er-As bonds must be broken and charge

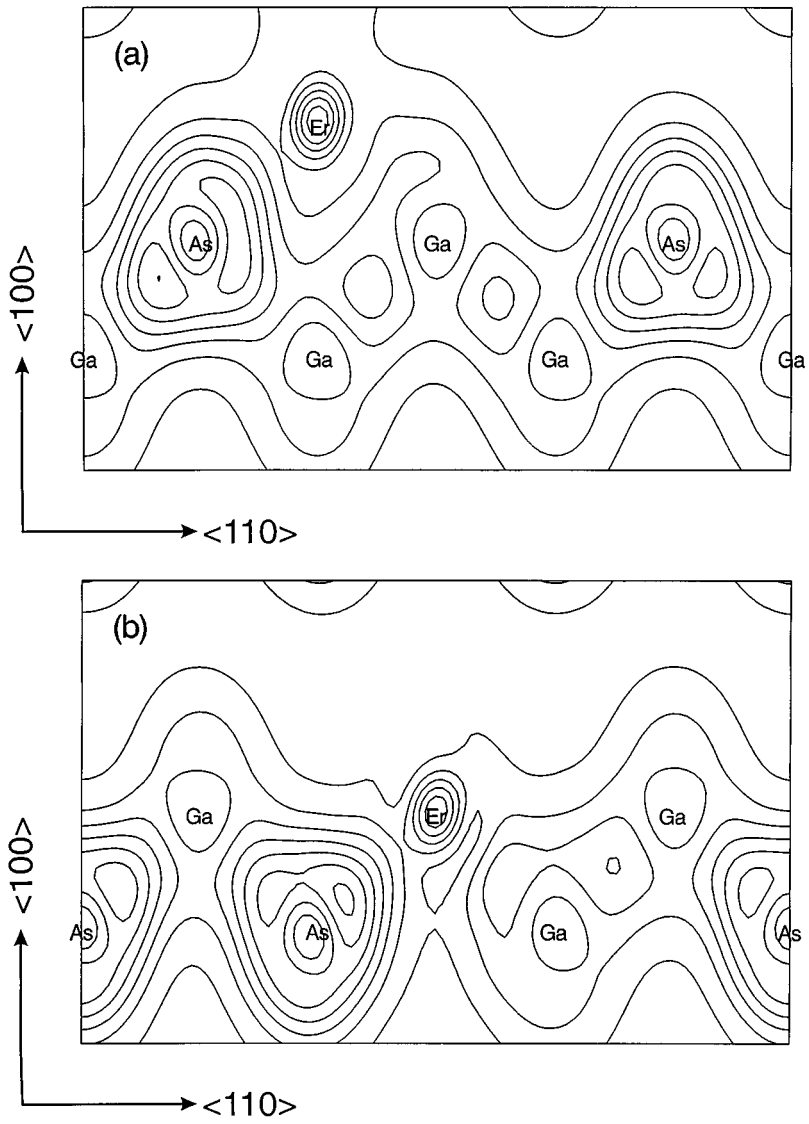

FIG. 12. Total valence charge distribution for (a) the coupled defect $\{Ga_{As}-Er_{i(As)}\}$ and (b) the coupled defect $\{Ga_{As}-Er_{Ga}\}$. There is a localized charge around $Er_{i(As)}$, which is similar to Fig. 3. The bond between $Er_{i(As)}$ and Ga_{As} is not clear. Er_{Ga} forms a bond with the neighboring As atom, but no bond with Ga_{As} is apparent.

localization around the Er atom must occur. Stress around the Er atom is reduced when the nearest-neighbor atom changes from As to Ga, but the breaking of the Er-As bond increases the total energy. As a result, the coupled defect is not stable.

The above investigations indicate that three mechanisms stabilize the coupled defects. One is lattice relaxation. The other two have a chemical nature. They are the formation of the Er-As bond and the charge transfer to the Er $5d$ orbital. This $5d$ orbital effect is characteristic of Er. Calculations of the total energy and investigations of the valence charge distribution indicate that the formation of the Er-As bond and the lattice relaxation are the main factors stabilizing the coupled defects. However, it is difficult to separate the chemical effect and the stress relaxation effect, since both modify the charge distribution.

In this paper, we discussed the coupling of one Er atom with one other point defect, and showed that Er tends to couple with native defects of GaAs. Complicated complexes including several Er atoms and point defects may be formed in actual GaAs:Er samples. Hence, even when a sample includes no impurities other than Er, various Er-related coupled defects could be formed, resulting in the complicated Er intra-$4f$-shell luminescence spectrum that depends on the growth conditions. To control Er luminescence centers in GaAs, it is necessary to control coupling between an Er atom and other impurities or defects. Impurities that form a strong bond with Er and reduce the lattice stress will form stable coupled defects. The reported coupled defects of Er with carbon[3] or with oxygen[4] may satisfy these requirements.

VI. CONCLUSIONS

We calculated the total energies of Er point defects and of Er defects coupled with other GaAs point defects. The calculations suggest that the coupled defects comprising Er coupled with other defects are formed depending on the growth conditions and the Fermi-level position. We found three mechanisms that stabilize the coupled defects. One is lattice relaxation. The other two have a chemical nature: the formation of the Er-As bond, and charge transfer to the Er $5d$ orbital. Investigations of the valence charge distribution show that the lattice relaxation and the formation of the Er-As bond are the main factors stabilizing the coupled defects.

The fact that Er tends to couple with other defects is probably the reason why the Er intra-4f-shell luminescence spectrum strongly depends on the sample preparation methods and growth conditions even when the sample contains very small amounts of other impurities.

ACKNOWLEDGMENTS

The authors are grateful to Professor Y. Horikoshi of Waseda University for many valuable discussions and to Dr. K. Takahei for his critical reading of the manuscript and fruitful discussions.

[1] A. Kozancki, M. Chan, C. Jeynes, B. Sealy, and K. Homewood, Solid State Commun. **78**, 763 (1991).

[2] J. Nakata, M. Taniguchi, and K. Takahei, Appl. Phys. Lett. **61**, 2665 (1992).

[3] A. Taguchi, K. Takahei, and J. Nakata, in *Rare Earth Doped Semiconductors*, edited by G. S. Pomrenke, P. B. Klein, and D. W. Langer, MRS Symposia Proceedings, No. 301 (Materials Research Society, Pittsburgh, 1993), p. 139.

[4] K. Takahei, A. Taguchi, Y. Horikoshi, and J. Nakata, J. Appl. Phys. **76**, 4332 (1994).

[5] M. Needels, M. Schlüter, and M. Lannoo, Phys. Rev. B **47**, 15 533 (1993).

[6] G. B. Bachelet, D. R. Hamann, and M Schlüter, Phys. Rev. B **26**, 4199 (1982).

[7] L. Kleinmann and D. M. Bylander, Phys. Rev. Lett. **48**, 1425 (1982).

[8] M. P. Teter, M. C. Payne, and D. C. Allan, Phys. Rev. B **40**, 12 255 (1989).

[9] O. Sugino and A. Oshiyama, Phys. Rev. Lett. **68**, 1858 (1992).

[10] M. Baeumler, J. Schneider, F. Köhl, and E. Tomzig, J. Phys. C **20**, L963 (1987).

[11] *Persons Handbook of Crystallographic Data for Intermetallic Phases* (American Society for Metals, Metals Park, 1985).

[12] E. Yamaguchi, K. Shiraishi, and T. Ohno, J. Phys. Soc. Jpn. **60**, 3093 (1991).

[13] S. J. Allen, Jr., N. Tabatabaie, C. J. Palmstrøm, G. W. Hull, T. Sands, F. DeRosa, H. L. Gilchrist, and K. C. Garrion, Phys. Rev. Lett. **62**, 2309 (1989); J. D. Ralston, H. Ennen, P. Wennekers, P. Hiesinger, N. Herres, J. Schneider, H. D. Müller, W. Tohtemund, F. Fuchs, J. Schmälzlin, and K. Thonke, J. Electron. Mater. **19**, 555 (1990).

[14] A. G. Petukhov, W. R. L. Lambrecht, and B. Segall, Phys. Rev. B **50**, 7800 (1994).

[15] G. A. Baraff and M. Schlüter, Phys. Rev. Lett. **55**, 1327 (1985).

[16] R. W. Jansen and O. F. Sankey, Phys. Rev. B **39**, 3192 (1989).

[17] U. Scherz and M. Scheffler, in *Density-Functional Theory of sp-Bonded Defects in III/V Semiconductors*, edited by E. W. Weber, Semiconductors and Semimetals Vol. 38 (Academic, New York, 1993).

[18] W. Walukiewicz, J. Vac. Sci. Technol. B **5**, 1062 (1987).

[19] A. Taguchi and T. Ohno, Mater. Sci. Forum **196–201**, 627 (1995).

[20] If the 2+ oxidation state of Er is stable, such charge transfer to the Er atom causes the change in the oxidation state from 3+ to 2+. We calculated the cohesive energy difference ΔE_{coh} for coupled defect $\{\mathrm{Er_{Ga}}-\mathrm{Ga}_{i(\mathrm{Ga})}\}$ in the same way described in Sec. III. The calculated value was +1.56 eV. This clearly shows that the Er^{3+} state is more stable than the Er^{2+} state in GaAs.